Pervasive mantle plume head heterogeneity: Evidence from the late Cretaceous Caribbean-Colombian oceanic plateau

Andrew C. Kerr,[1] John Tarney,[2] Pamela D. Kempton,[3] Piera Spadea,[4] Alvaro Nivia,[5] Giselle F. Marriner,[6] and Robert A. Duncan[7]

Received 10 July 2001; revised 8 January 2002; accepted 13 January 2002; published 24 July 2002.

[1] In SW Colombia picritic pillow lavas and tuffs, as well as breccias composed of picritic clasts, occur interspersed with basalts of the Central Cordillera and represent accreted portions of the ~90 Ma Colombian/Caribbean oceanic plateau (CCOP). We present new geochemical data for these picrites and high-MgO basalts from SW Colombia, along with new data from Deep Sea Drilling Project Leg 15 drill sites. The $^{40}Ar/^{39}Ar$ ages for the CCOP in the Central Colombian Cordillera range from 87 to 93 Ma. Both SW Colombia picrites and Leg 15 basalts are compositionally diverse and range from reasonably enriched ($(La/Nd)_n > 1$ and $(\varepsilon_{Nd})_i < +4.1$) to relatively depleted ($(La/Nd)_n < 1$ and $(\varepsilon_{Nd})_i > +8.0$). Nb/Y and Zr/Y systematics suggest that the depleted component is not depleted MORB mantle, but is an intrinsic part of the plume. The bulk of the CCOP compositions can be explained by mixing between this depleted mantle and a HIMU component. However, radiogenic isotope systematics indicate the presence of an EM2 (or possibly EM1) component within the plume. Mantle melt modeling suggests that the enriched magma types are the product of deeper, small degree melting of a pervasively heterogeneous plume comprising a refractory matrix with enriched streaks/blobs, whereas shallower, more extensive melting, results in the formation of relatively depleted magmas. *INDEX TERMS:* 8121 Tectonophysics: Dynamics, convection currents and mantle plumes; 1040 Geochemistry: Isotopic composition/chemistry; 3640 Mineralogy and Petrology: Igneous petrology; 1025 Geochemistry: Composition of the mantle; 3670 Mineralogy and Petrology: Minor and trace element composition; *KEYWORDS:* mantle plume, mantle melting, oceanic plateau, picrite, komatiite, Colombia

1. Introduction

[2] Our knowledge of oceanic plateaus comes mainly from three Cretaceous age plateaus: the Ontong Java plateau in the western Pacific [e.g., *Mahoney et al.*, 1993], the Kerguelen plateau in the Indian Ocean [*Weis et al.*, 1989; *Frey et al.*, 2000] and the Caribbean-Colombian plateau [*Donnelly et al.*, 1990; *Kerr et al.*, 1996a, 1996b, 1997a, 1997b]. With the exception of small obducted fragments the former two plateaus have only been sampled in a few Ocean Drilling Program (ODP) drill holes. In the Ontong Java, compositional variability is quite limited [*Mahoney et al.*, 1993]. However, Kerguelen plateau is compositionally diverse, and recent drilling results [*Frey et al.*, 2000] have confirmed suggestions that part of the plateau is underlain by ancient continental lithosphere. In contrast, the Caribbean-Colombian oceanic plateau is well exposed around the margins of the Caribbean and in accreted fragments in NW South America [*Kerr et al.*, 1997a, 1997b]. It is not underlain by any known continental lithospheric fragments, yet has been shown to locally display significant compositional diversity [*Kerr et al.*, 1996a, 1997a; *Hauff et al.*, 2000a, 2000b].

[3] In this paper we present new elemental, isotopic (Sr, Nd, and Pb), and $^{40}Ar/^{39}Ar$ age data for compositionally heterogeneous picrites and basalts from the Central Cordillera of Colombia. Additionally, we report new trace element data from basalts drilled during Deep Sea Drilling Project (DSDP) Leg 15. All these samples extend both the geochemical range and the geographical extent of heterogeneity displayed by the plateau lavas [*Kerr et al.*, 1996a, 1996b; *Sinton et al.*, 1998]. We will demonstrate that this heterogeneity is not localized but seems to be ubiquitous throughout the whole province, usually where high-MgO lavas occur. We will explore the nature, possible origin, and partial melting of these plume source components.

1.1. Caribbean-Colombian Oceanic Plateau (CCOP)

[4] Recent geochemical work has shown that the vast majority of accreted oceanic material in western Colombia are fragments of mantle plume-derived, obducted oceanic

[1]Department of Earth Sciences, Cardiff University, Cardiff, UK.
[2]Department of Geology, University of Leicester, Leicester, UK.
[3]NERC Isotope Geosciences Laboratory, Nottingham, UK.
[4]Dipartimento di Georisorse E Territorio, Università Degli Studi di Udine, Udine, Italy.
[5]Ingeominas–Regional Pacifico, Cali, Colombia.
[6]Department of Geology, Royal Holloway University of London, Egham, UK.
[7]College of Oceanography, Oregon State University, Corvallis, Oregon, USA.

Copyright 2002 by the American Geophysical Union.
0148-0227/02/2001JB000790$09.00

plateau [*Millward et al.*, 1984; *Kerr et al.*, 1997a, 1997b; *Sinton et al.*, 1998]. Remnants of the same plateau also comprise most of the Caribbean plate and are exposed around its margins [*Donnelly et al.*, 1990; *Kerr et al.*, 1996b, 1997b; *Sinton et al.*, 1998; *Lapierre et al.*, 2000]. Additionally, the submerged portion of the plateau was sampled during drilling by DSDP/ODP Legs 15 and 163 in the Caribbean Sea [*Donnelly et al.*, 1973; *Sinton et al.*, 2000].

[5] The CCOP consists of material of at least two, and possibly three, broadly different ages: an Aptian age (124–112 Ma) phase [*Lapierre et al.*, 2000], a 91–83 Ma phase (the most voluminous) and a 78–72 Ma phase. Thus in addition to there being a major phase of oceanic plateau formation in the Cretaceous western Pacific [cf. *Mahoney et al.*, 1993; *Neal et al.*, 1997], there was also a significant phase of oceanic plateau construction in the eastern Pacific, of which the CCOP is the residual part. Accretion of this former Pacific plateau against the continental margin of South America, and insertion into the Caribbean region, has locally exposed the lower crustal layers of the plateau [*Nivia*, 1996; *Kerr et al.*, 1997b, 1998].

[6] High-MgO lavas are found at intervals throughout the CCOP [*Kerr et al.*, 1996a, 1996b; *Alvarado et al.*, 1997; *Hauff et al.*, 2000b], including the komatiites of Gorgona Island, Colombia [*Kerr et al.*, 1996a; *Arndt et al.*, 1997]. This paper focuses on some of the less well characterized occurrences of picrite and high-MgO basalt in south west Colombia, which are geochemically distinct from most of the high-MgO lavas in the rest of the province.

1.2. Geologic Setting and Age of Colombian High-MgO Lavas

[7] All of the high-MgO lavas (>12 wt %) are found in small ophiolitic associations in southwestern Colombia along the major terrane boundary of the Romeral fault zone [*Spadea et al.*, 1989] (Figure 1). In Colombia the accreted plateau material is exposed in three approximately N-S trending belts: the Serranía de Baudó, the Western Cordillera, and the Central Cordillera. The picrites and high-MgO basalts of the Romeral fault zone lie within the Central Cordillera and the eastern part of the Western Cordillera (Figure 1).

[8] The CCOP basalts of the Pacific coast and the Western Cordillera are of two distinct ($^{40}Ar/^{39}Ar$) ages: 72–78 Ma and 90–92 Ma [*Kerr et al.*, 1997a; *Sinton et al.*, 1998]. Prior to this study the only constraint on the age of the igneous rocks of the Central Cordillera was the arc-related Buga batholith that intrudes the plateau sequence of the Central Cordillera. K-Ar dating of this batholith gives an age range of 114–69 Ma, which has also yielded a Rb-Sr isochron age of 99 ± 4 Ma [*McCourt et al.*, 1984]. On the basis of these ages from the Buga batholith, *McCourt et al.* [1984] proposed that the basalts and picrites of the Central Cordillera were significantly older than 100 Ma. However, we have been able to obtain reliable Ar-Ar step-heating plateau ages (with atmospheric $^{40}Ar/^{36}Ar$ intercepts) for two high-MgO lavas from the Central Cordillera of SW Colombia. Sample COL 354, a picritic glass from Rio Boloblanco, gave a plateau age of 93.21 ± 3.60 Ma (2 SD), whereas sample COL 436 from El Encenillo gave a whole rock plateau age of 88.95 ± 3.27 Ma (2 SD). (See Figures A1 and A2, available as electronic supporting data,[1] for plateau and isochron diagrams.)

[9] On the basis of the 99 Ma crosscutting batholith age and slightly different chemical signatures, *Kerr et al.* [1997a] speculated that the igneous rocks of the Central Cordillera may have been of Aptian age (124–112 Ma). However, the 93–89 Ma ages obtained for the high-MgO lavas of the Central Cordillera place doubt on the validity of the Rb-Sr age for the Buga batholith, and there is a pressing need to resolve the age relationship between the lavas and the Buga batholith.

1.3. Field Relations

[10] The rocks of the Central Cordillera are less well exposed and generally more altered than those of the Western Cordillera and the Serranía de Baudó. The main sequence of basaltic igneous rocks in the Central Cordillera is known as the Amaime Formation and consists of imbricated slices of basalts teconically interlayered with clastic metasediments [*Kerr et al.*, 1997a]. Just south of the Amaime Formation, smaller exposures of ultramafic/mafic oceanic crustal material crop out along the Romeral fault zone (Figure 1) and are briefly detailed below. Full descriptions are available from *Spadea et al.* [1989].

[11] The El Penol-El Tambo ophiolitic succession (Figure 1) consists of a thrust zone of basalts, gabbros, dolerites, and plagiogranites, with minor picrites. The high-MgO rocks from El Encenillo consist of tuff breccias or agglomerates interlayered within a sequence of basaltic and picritic breccias, basaltic pillow lavas and hyaloclastites, which are intruded by basaltic dikes. Several picritic pillow lavas outcrop at one locality in the Rio Boloblanco valley (Figure 1).

[12] The Los Azules complex (Figure 1) is 30 km long × ~5 km wide and is composed of mafic/ultramafic plutonic rocks and high-MgO pillow lavas, intruded by basaltic dikes. The ophiolitic rocks of the La Tetilla complex outcrop discontinuously over an area of 50 km^2, NW of Popayán (Figure 1), and are composed of massive basalt flows, dolerites, breccias, isotropic gabbros, and cumulus wehrlite, all intruded by dolerite dikes. The La Vetica area, SSW of Cali (Figure 1), comprises volcanogenic siltstone, sandstone, and microbreccia, with interlayered pillow lavas.

1.4. Alteration and Petrography

[13] The extrusive high-MgO rocks of the Central Cordillera display variable degrees of alteration and metamorphism, from prehnite-pumpellyite to greenschist facies assemblages. *Kerr et al.* [1997a] have shown that the most mobile elements in CCOP lavas from Colombia were Na, K, Rb, Ba, and Sr, whereas the high field strength elements were relatively immobile. The related picrites and high-MgO basalts of the present study display similar trends in elemental mobility.

[14] The petrography and mineral chemistry of the samples are detailed by *Spadea et al.* [1989]. Briefly, olivine

[1] Supporting $^{40}Ar/^{39}Ar$ data Figures A1 and A2 and major and trace element data Tables A1 and A2 are available via Web browser or via Anonymous FTP from ftp://agu.org, directory "apend" (Username = "anonymous", Password = "guest"); subdirectories in the ftp site are arranged by paper number. Information on searching and submitting electronic supplements is found at http://www.agu.org/pubs/esupp_about.html.

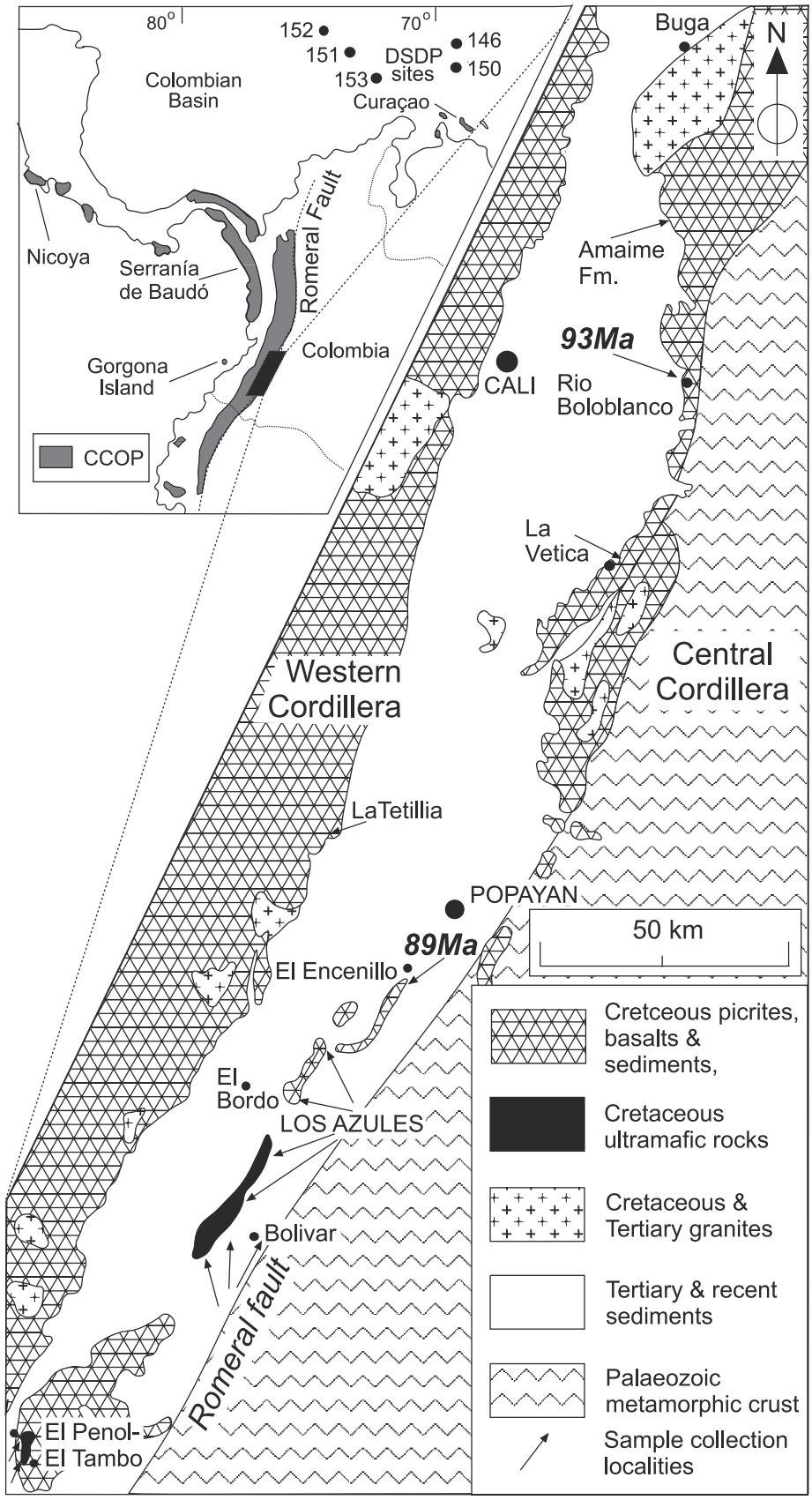

Figure 1. Map of western Colombia showing the broad locations of samples collected for this study. The smaller map shows the locations of other exposed portions of the Caribbean- Colombian Cretaceous oceanic plateau.

textures in the picrites and high-MgO basalts of the Central Cordillera vary from microspinifex phenocrysts to coarse (up to 5 mm), hollow olivine phenocrysts which range in composition from Fo_{87-89} (Rio Boloblanco) to Fo_{88-91} (Los Azules) [*Spadea et al.*, 1989]. These zoned olivine phenocrysts would have been in equilibrium with a magma containing 14–18 wt % MgO. Furthermore, calculations using the liquid Ni content (after the method of *Korenaga and Kelemen* [2000]) also suggest that the MgO content of the primary mantle melt was close to 15 wt %. Thus samples with >18–20 wt % MgO (Table 1 and Figure 2) contain accumulated olivine. Assuming an olivine composition of Fo_{90}, our calculations suggest that the picrites with 20–30 wt % MgO contain 20–45 vol % accumulated olivine (Figure 2c).

2. Geochemistry

2.1. Analytical Procedures

[15] Major and trace elements (Tables 1, A1, and A2) were analyzed by X-ray fluorescence at Leicester University using conventional techniques (see *Kerr et al.* [1997a] for further details). Rare earth elements (Tables 1, A1, and A2) were analyzed by Inductively Coupled Plasma-Atomic Emission Spectroscopy at Royal Holloway [see Walsh et al., 1981]. (Tables A1 and A2 are available as electronic supporting data.)

[16] Sr, Pb, and Nd isotopes (Table 2) were analyzed using a Finnegan MAT 262 multicollector mass spectrometer at the NERC Isotope Geosciences Laboratory (NIGL). Blanks for Sr, Nd, and Pb were less than 194, 76, and 172 pg, respectively. Reference standards throughout the course of analysis averaged values of $^{87}Sr/^{86}Sr = 0.710182 \pm 14$ (1σ) for the NBS 987 standard, $^{143}Nd/^{144}Nd = 0.511890 \pm 6$ (1 σ) for the La Jolla Nd standard. The ratio $^{87}Sr/^{86}Sr$ was normalized during run time to $^{86}Sr/^{88}Sr = 0.1194$; $^{143}Nd/^{144}Nd$ was normalized to a value of $^{146}Nd/^{144}Nd = 0.7219$. Sample data are reported relative to accepted values of NBS 987 of 0.71024 and 0.51186 for La Jolla. On the basis of repeated runs of NBS 981 the reproducibility of Pb-isotope ratios is better than ±0.1%. Pb isotope ratios were corrected relative to the average standard Pb isotopic compositions of *Todt et al.* [1993]. All samples were acid-leached prior to dissolution. See *Kempton* [1995] and *Royse et al.* [1998] for further analytical details.

[17] Age determinations were performed at Oregon State University using standard $^{40}Ar/^{39}Ar$ incremental heating techniques [*Duncan and Hargraves*, 1990; *Duncan and Hogan*, 1994]. Neutron flux during irradiation was monitored by FCT-3 biotite (27.7 Ma [*Hurfurd and Hammerschmidt*, 1985]). Plateau ages were calculated from consecutive steps that are concordant within 2σ error using the procedure described by *Dalrymple et al.* [1988], in which step ages were weighted by the inverse of their variance. See *Sinton et al.* [1998] for further details.

2.2. Colombian Basalts and Picrites

2.2.1. Major and trace elements

[18] The lavas of the southern Central Cordillera of Colombia range in composition from basalts to picrites, some of which contain over 30 wt % MgO (Figure 2). As will be shown below, four groups can be identified using trace element ratios; however, these four groups are not readily apparent from an inspection of Al_2O_3, CaO and alkali contents (Table 1 and Figure 2). Three groups can be identified on the basis of TiO_2 contents and are broadly defined on Harker-type diagrams by the trends for the El Encenillo and Los Azules samples, with the El Encenillo trend being more enriched in TiO_2 and P_2O_5 than the Los Azules samples (Figure 2a). Additionally, some samples from Los Azules define a third trend (ringed on Figures 2a, 2c, and 2d) which is more similar (or intermediate) in composition to the El Encenillo trend.

[19] Figures 2c and 2d show that rocks which display the more enriched El Encenillo trend contain over 21 ppm Nb and over 150 ppm Zr (at <15 wt % MgO), whereas rocks with the more depleted Los Azules trend contain <10 ppm Nb and <90 ppm Zr (at <15 wt % MgO). The intermediate group between the El Encenillo and Los Azules samples is clearly evident on Figures 2c and 2d. The former group can be most clearly distinguished on a plot of $(La/Nd)_n$ versus Nb/Y (Figure 3), where it again occupies a position between the El Encenillo and Los Azules samples (Nb/Y 0.55–0.65 and $(La/Nd)_n > 1.0$). Figure 3 also clearly shows a fourth group of samples which is characterized by a more depleted signature (Nb/Y < 0.25 and $(La/Nd)_n < 0.9$) relative to the other Colombian samples. On Figure 3 each of the compositional types is labeled 1 to 4, with type 1 being the most enriched and type 4 the most depleted.

[20] Mantle-normalized multielement diagrams are shown on Figure 4. In order to minimize the effect of elemental dilution due to of olivine accumulation, samples have been placed into groups defined by relatively small MgO ranges. The marked compositional variability of the basalts and picrites, even within restricted MgO ranges, is noteworthy. Samples with more enriched incompatible trace element contents, characterized by the samples from El Encenillo, have steeper primitive-mantle-normalized patterns ($(Sm/Yb)_n > 2$; Ti/Y > 550; Figures 4 and 5) than the rest of the samples, which have flatter patterns ($(Sm/Yb)_n = 1–2$; Ti/Y < 500; Figures 4 and 5). As noted above, while most of the analyzed samples possess $(La/Nd)_n > 1$, some of the Los Azules and El Penol-El Tambo samples possess $(La/Nd)_n < 1.0$ (Figures 4 and 5a). These light rare earth element (LREE)-depleted samples also have Zr/Nb > 15 and $(Sm/Yb)_n$ 1–2 (Figures 5a and 5b).

2.2.2. Radiogenic isotopes

[21] The enriched and depleted groups identified on the basis of their trace element contents and ratios also possess characteristic radiogenic isotope ratios (Figures 5 and 6). On Figures 5c and 5d, plots of $(\varepsilon_{Nd})_i$ against $(La/Nd)_n$ and $(Sm/Yb)_n$ (where i = 90 Ma) show that LREE-enriched samples from El Encenillo have $(\varepsilon_{Nd})_i$ values of +3.6 to +4.1, whereas samples with chondritic and depleted LREE patterns have $(\varepsilon_{Nd})_i > 6.0$ (Figure 5c). Figure 5c also reveals that two samples from Los Azules (COL 547 and COL 472) are more enriched in the LREE than samples with similar $(\varepsilon_{Nd})_i$, such that they plot off the main sample trend. It is noteworthy that on Figure 5d the samples from Los Azules plot at higher $(Sm/Yb)_n$ values than other CCOP lavas.

[22] On the $(\varepsilon_{Nd})_i$ versus $(^{87}Sr/^{86}Sr)_i$ diagram (Figure 6a) the Colombian high-MgO samples define a negative trend. The three trace element-enriched samples from El Encenillo

Table 1. Representative Major and Trace Element Data for Southwest Colombian Picrites[a]

	Sample																		
	257770	257771	COL435	COL436	COL437	COL354	COL355	COL468	COL469	COL472	COL474	COL541	COL547	COL301	COL311	COL166	COL530	COL536	COL537
Locality	LT	LT	EE	EE	EE	RB	RB	LAZ	LAZ	LAZ	LAZ	LAZ	LAZ	EP-ET	EP-ET	RC	LV	LV	LV
SiO_2	52.61	50.13	42.47	47.63	50.37	46.97	46.50	48.89	49.85	48.81	44.62	48.77	46.73	49.74	51.05	43.77	47.65	47.30	53.34
TiO_2	1.04	0.99	2.86	2.40	2.49	0.74	0.71	1.51	1.53	0.89	0.87	1.39	1.22	2.06	0.74	1.24	0.81	0.80	2.82
Al_2O_3	13.91	14.17	11.53	11.52	13.11	9.73	9.52	14.59	14.53	12.86	6.15	12.52	12.00	17.95	14.69	10.04	12.96	10.77	11.36
Fe_2O_3[b]	10.15	10.79	17.11	13.53	10.92	11.30	11.17	11.72	11.55	10.66	12.27	12.95	13.56	8.02	9.63	12.94	10.37	11.30	11.00
MnO	0.17	0.17	0.20	0.19	0.13	0.17	0.17	0.18	0.18	0.17	0.17	0.18	0.21	0.14	0.16	0.20	0.16	0.17	0.14
MgO	8.80	9.41	17.20	13.75	9.45	20.81	21.37	8.88	9.18	11.55	27.83	10.31	9.53	9.88	9.29	23.86	13.89	16.89	7.26
CaO	11.68	11.72	7.20	7.40	8.03	7.81	7.97	10.68	9.87	11.61	7.25	10.82	12.38	7.55	12.17	8.19	13.32	9.67	8.90
Na_2O	1.52	1.50	0.60	1.95	3.31	0.43	0.82	2.21	2.34	2.91	0.05	2.00	2.14	2.22	1.85	0.04	0.58	0.83	4.07
K_2O	0.12	0.08	0.20	0.14	0.91	0.07	0.06	0.44	0.55	0.08	0.02	0.30	0.46	1.16	0.09	0.01	0.17	0.05	0.12
P_2O_5	0.09	0.08	0.35	0.26	0.31	0.05	0.05	0.19	0.19	0.09	0.12	0.11	0.16	0.33	0.06	0.08	0.06	0.08	0.21
Total[c]	100.08	99.03	99.72	98.76	99.04	98.08	98.35	99.30	99.78	99.63	99.34	99.35	98.47	99.05	99.74	100.36	99.96	97.85	99.20
LOI	1.24	2.68	5.43	4.55	0.23	3.29	3.03	3.11	1.87	3.03	6.20	3.10	2.91	3.61	0.94	6.67	4.64	5.45	2.37
Sc	38.6	41.0	19.7	23.4	26.7	32.5	29.0	33.2	29.6	30.8	20.0	37.6	32.7	22.5	39.2	22.4	43.5	31.3	28.8
V	278	271	214	241	242	202	188	362	345	334	157	366	334	153	240	249	251	228	367
Cr	414	454	1086	955	496	2015	2055	463	434	1393	2115	671	451	352	485	999	877	1462	514
Ba	56	51	126	57	105	27	24	128	126	85	17	77	332	738	31	10	88	46	53
Nb	5.4	5.1	28.5	20.1	23.6	2.6	2.9	8.7	8.7	2.2	6.1	5.1	13.3	12.4	2.3	3.4	3.2	4.7	16.9
Zr	54	52	194	162	159	36	33	97	90	40	37	72	60	111	35	63	43	44	148
Y	19.1	17.8	25.2	25.0	22.6	12.5	13.0	26.0	24.3	19.0	9.3	22.5	20.7	21.0	16.6	19.9	17.1	16.0	26.9
Sr	126	126	196	301	206	78	104	335	247	398	30	225	282	478	131	29	57	56	877
Rb	3.2	2.8	4.1	3.5	15.8	2.7	2.2	7.9	10.3	1.9	3.7	6.1	12.6	16.6	2.0	0.9	4.1	1.8	1.9
Ga	14.0	14.5	21.0	19.2	17.5	11.5	11.3	20.6	22.3	14.3	7.5	17.1	16.9	14.7	15.3	8.2	13.4	12.4	22.1
Ni	135	147	1038	707	190	913	937	219	209	264	1523	265	168	149	136	359	306	641	165
La	4.03	2.70	19.62	12.32	18.04	–	2.34	6.08	5.51	2.42	3.51	3.29	7.52	19.80	2.06	2.61	2.85	3.31	11.31
Ce	10.62	11.60	47.10	31.33	43.63	–	6.19	15.54	14.77	6.33	8.39	9.71	15.19	44.21	5.46	7.83	7.79	8.16	30.80
Pr	1.36	–	5.84	4.10	5.31	–	0.82	2.23	2.14	0.92	1.02	1.48	1.79	5.26	0.69	1.04	1.04	1.01	4.11
Nd	7.37	6.40	24.48	18.18	22.36	–	4.56	11.42	10.99	5.58	5.09	8.41	9.08	21.30	4.84	6.59	5.65	5.59	20.59
Sm	1.96	1.82	5.26	4.28	4.75	–	1.17	3.07	3.01	1.76	1.35	2.29	2.25	3.89	1.27	1.99	1.58	1.49	5.10
Eu	0.75	–	1.82	1.55	1.68	–	0.49	1.20	1.14	0.74	0.47	0.91	0.89	1.34	0.54	0.77	0.62	0.57	1.83
Gd	2.56	–	5.38	4.62	5.08	–	1.72	3.93	3.91	2.67	1.63	3.22	2.94	3.87	1.96	2.64	2.28	2.04	5.67
Dy	2.82	–	4.29	3.90	4.07	–	1.88	3.95	3.93	2.92	1.60	3.23	3.20	3.76	2.42	2.81	2.56	2.19	5.05
Ho	0.58	–	0.77	0.71	0.78	–	0.40	0.78	0.78	0.58	0.31	0.64	0.62	0.75	0.50	0.54	0.55	0.44	0.91
Er	1.52	–	1.70	1.61	1.44	–	0.99	1.94	1.92	1.44	0.77	1.42	1.56	1.84	1.42	1.37	1.50	1.17	2.03
Yb	1.58	–	1.46	1.43	1.52	–	1.08	1.84	1.82	1.36	0.75	1.46	1.49	1.91	1.48	1.31	1.62	1.24	1.71
Lu	0.29	–	0.22	0.22	0.25	–	0.18	0.29	0.29	0.21	0.11	0.24	0.23	0.31	0.24	0.20	0.27	0.22	0.25
Th	0.30	0.25	–	–	1.98	–	–	–	–	bd	–	2.09	0.55	–	–	–	–	–	–
Pb	0.72	bd	–	–	1.18	–	–	–	–	0.22	–	2.43	2.04	–	–	–	–	–	–

[a]LT, La Tetilla; EE, El Encenillo; RB, Rio Boloblanco; LAZ, Los Azules; EP-ET, El Penol-El Tambo; RC, Rio Chapungo; LV, La Vetica; bd, below detection.
[b]All iron reported as Fe_2O_3.
[c]Totals reported on a dry basis.

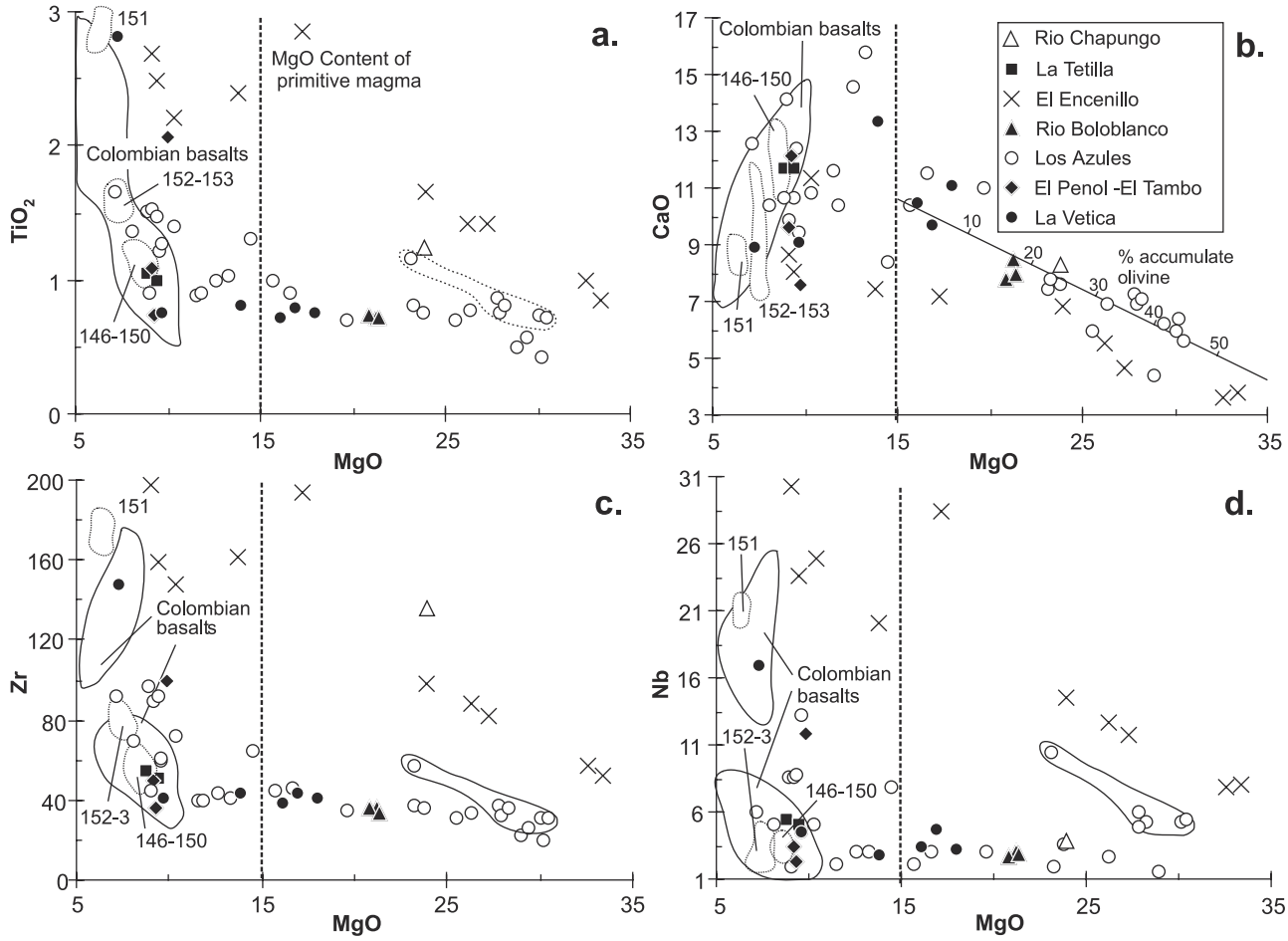

Figure 2. Plots of major and trace elements against MgO showing the composition of picritic and high MgO samples from SW Colombia. The field for other Colombian basalts is taken from *Kerr et al.* [1997a]. The dashed fields represent samples from DSDP Leg 15 Sites 146, 150, 151, 152, and 153 (Table A2). The vertical dashed lines indicate estimated primitive magma compositions for the Central Cordillera lavas. The dashed ringed Los Azules samples are discussed in the text.

form a distinct group with $(\varepsilon_{Nd})_i$ and $(^{87}Sr/^{86}Sr)_i$ ranging from +3.6 to +4.1 and from 0.7035 to 0.7038, respectively. Sample COL 537 (from La Vetica), which is enriched in incompatible trace elements like the El Encenillo samples, also possesses a relatively low $(\varepsilon_{Nd})_i$ of +6.0. With the exception of COL 541 and COL 472, ($(\varepsilon_{Nd})_i$ of +8.8 and +11.0, respectively) the rest of the samples from Los Azules, El Penol-El Tambo, Rio Chapungo, and La Tetilla have a restricted range of $(\varepsilon_{Nd})_i$ from +6.9 to +8.3, and a slightly wider range in $(^{87}Sr/^{86}Sr)_i$ of 0.70315 to 0.70381.

[23] Pb isotope systematics generally parallel the trends observed for Nd isotopes (Figure 6), in that the one El

Table 2. Sr, Nd, and Pb Radiogenic Isotope Analyses of High-MgO Basalts and Picrites From SW Colombia

	$^{87}Sr/^{86}Sr^a$	$(^{87}Sr/^{86}Sr)_i^b$	$^{143}Nd/^{144}Nd^a$	$(\varepsilon_{Nd})_i^b$	$^{206}Pb/^{204}Pb^a$	$^{207}Pb/^{204}Pb^a$	$^{208}Pb/^{204}Pb^a$
257770	0.703371	0.703277	0.512884	6.93	19.026	15.558	38.741
257771	0.703347	0.703265	0.512880	6.86	19.228	15.597	39.082
COL435	0.703937	0.703860	0.512722	3.79	–	–	–
COL436	0.703671	0.703628	0.512712	3.59	–	–	–
COL437	0.703894	0.703565	0.512738	4.12	19.684	15.59	39.502
COL355	0.703249	0.703171	0.512911	7.46	–	–	–
COL468	0.703580	0.703493	0.512954	8.29	–	–	–
COL469	0.703490	0.703336	0.512938	7.99	19.441	15.561	38.985
COL472	0.702948	0.702930	0.513092	10.98	19.327	15.576	38.858
COL541	0.703229	0.703129	0.512980	8.80	18.555	15.591	38.442
COL547	0.703446	0.703281	0.512927	7.78	19.624	15.615	39.263
COL311	0.703880	0.703827	0.512955	8.32	–	–	–
COL537	0.703289	0.703251	0.512840	6.08	–	–	–

[a]Measured values.
[b]The *i* values are age corrected to 90 Ma.

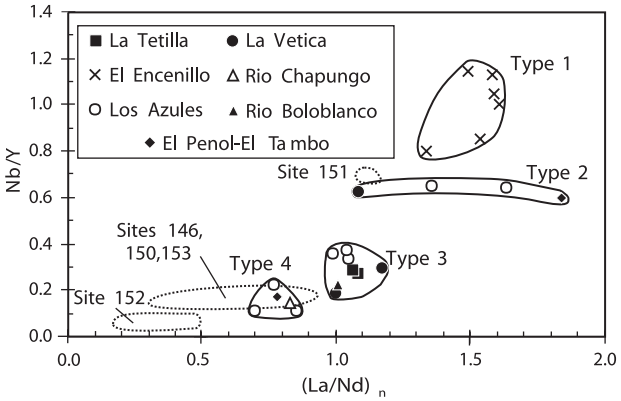

Figure 3. Plot of Nb/Y versus $(La/Nd)_n$ showing the picrites and high-MgO samples from SW Colombia along with fields for Leg 15 basalts. The samples can be subdivided into four different magma types.

Encenillo sample analyzed for Pb isotopes (COL 437) possesses the highest measured $^{208}Pb/^{204}Pb$ and $^{206}Pb/^{204}Pb$ ratios (39.5 and 19.7, respectively; Figure 6), while a more depleted Los Azules sample (COL 541) has the lowest $^{208}Pb/^{204}Pb$ and $^{206}Pb/^{204}Pb$ ratios (33.9 and 18.6, respectively; Figure 6). However, simple two-component mixing cannot explain all the lead isotope systematics (see Figures 6b–6d) and a third (relatively enriched) component seems to be required, particularly when published CCOP isotope data are also plotted. This third component is characterized by $^{206}Pb/^{204}Pb$ of 19.1 to 19.5, $^{207}Pb/^{204}Pb$ of 15.60 to 15.65, and $(\varepsilon_{Nd})_i$ of +3 to −1.

2.3. Comparison With Data From DSDP Leg 15

[24] Table A2 and Figures 2, 5, and 6 present new elemental data from basalts drilled during DSDP Leg 15 in the Caribbean Seafloor and this complements other recently published data [*Sinton et al.*, 1998; *Hauff et al.*, 2000a]. The samples from DSDP Site 151 possess elevated levels of incompatible trace elements that are similar to those from El Encenillo and other more-enriched CCOP samples (Figure 3). All other lavas from Leg 15 are LREE depleted. Incompatible trace element ratios ($(La/Nd)_n$ and Nb/Y; Figure 3) can be used to divide the these depleted samples into two groups, one consisting of lavas from Sites 146, 150, and 153 and a second more depleted group from Site 152.

[25] This threefold subdivision is also evident from the limited number of isotopic analyses available (Table A2 and Figures 5c, 5d, and 6a [*Hauff et al.*, 2000a]). The more enriched (Site 151) sample has an $(\varepsilon_{Nd})_i$ of +5.1, whereas the most depleted Site 152 sample possesses an $(\varepsilon_{Nd})_i$ value of +9.4. The sample from Site 146, which in terms of trace elements lies between Sites 151 and 152, also possesses Nd and Sr isotopic characteristics which are intermediate between the samples from Sites 151 and 152 (Figure 6a). It should be noted that the basalts drilled at Site 152 are significantly younger (Campanian; 73–84 Ma) than those from the other drill sites [*Sinton et al.*, 1998, 2000].

2.4. Comparisons With Other CCOP Sections

[26] The most notable feature of the picrites and basalts from this region of SW Colombia is the wide compositional range displayed by the radiogenic isotopes and trace elements, in comparison with most of the rest of the CCOP of a similar age (93–86 Ma) (Figures 5–7). This is particularly well demonstrated by $(\varepsilon_{Nd})_i$ values, with most of the CCOP basalts, particularly from Colombia, Curaçao [*Kerr et al.*, 1996b], and Nicoya, Costa Rica [*Sinton et al.*, 1997; *Hauff et al.*, 1997, 2000b], possessing a relatively restricted range of $(\varepsilon_{Nd})_i$ from +6 to +8.5, along with flat, to slightly enriched, chondrite-normalized REE patterns (Figures 5c and 6). Most of the less depleted Los Azules, La Tetilla, and La Vetica samples fall within this range.

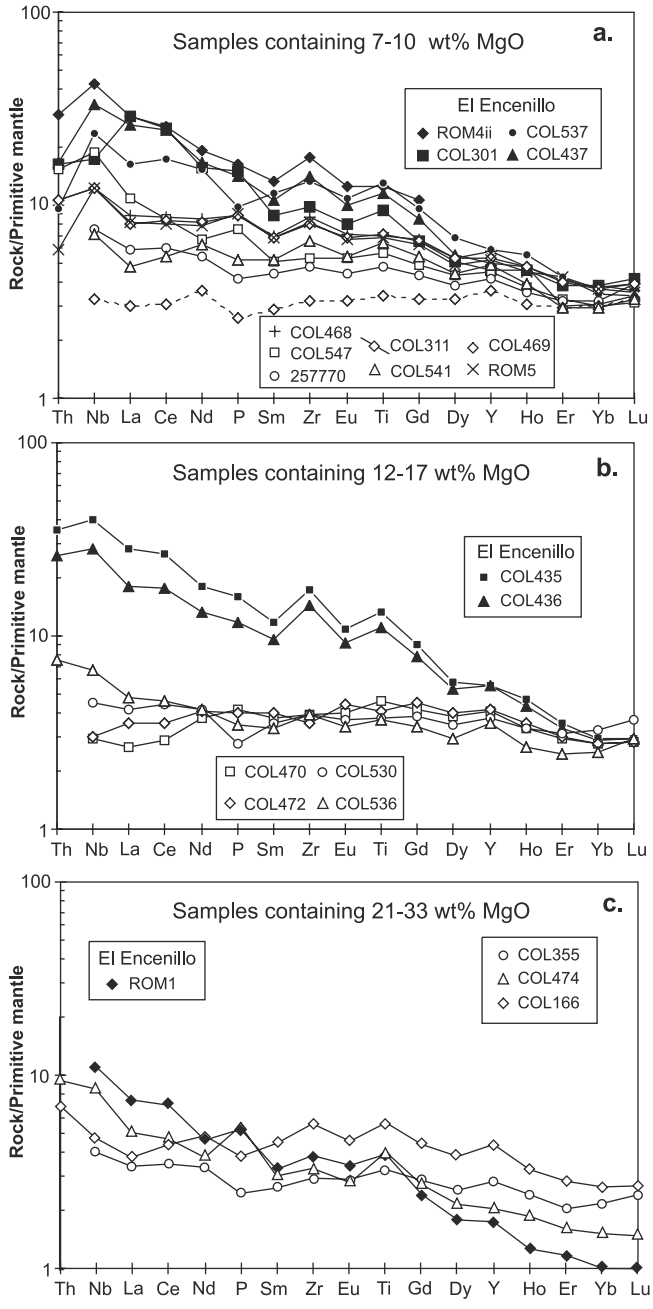

Figure 4. Primitive mantle normalized multielement plots, with samples grouped into three ranges of MgO: (a) 7–10 wt %, (b) 12–17 wt %, and (c) 21–33 wt %. Normalizing values are from *Sun and McDonough* [1989].

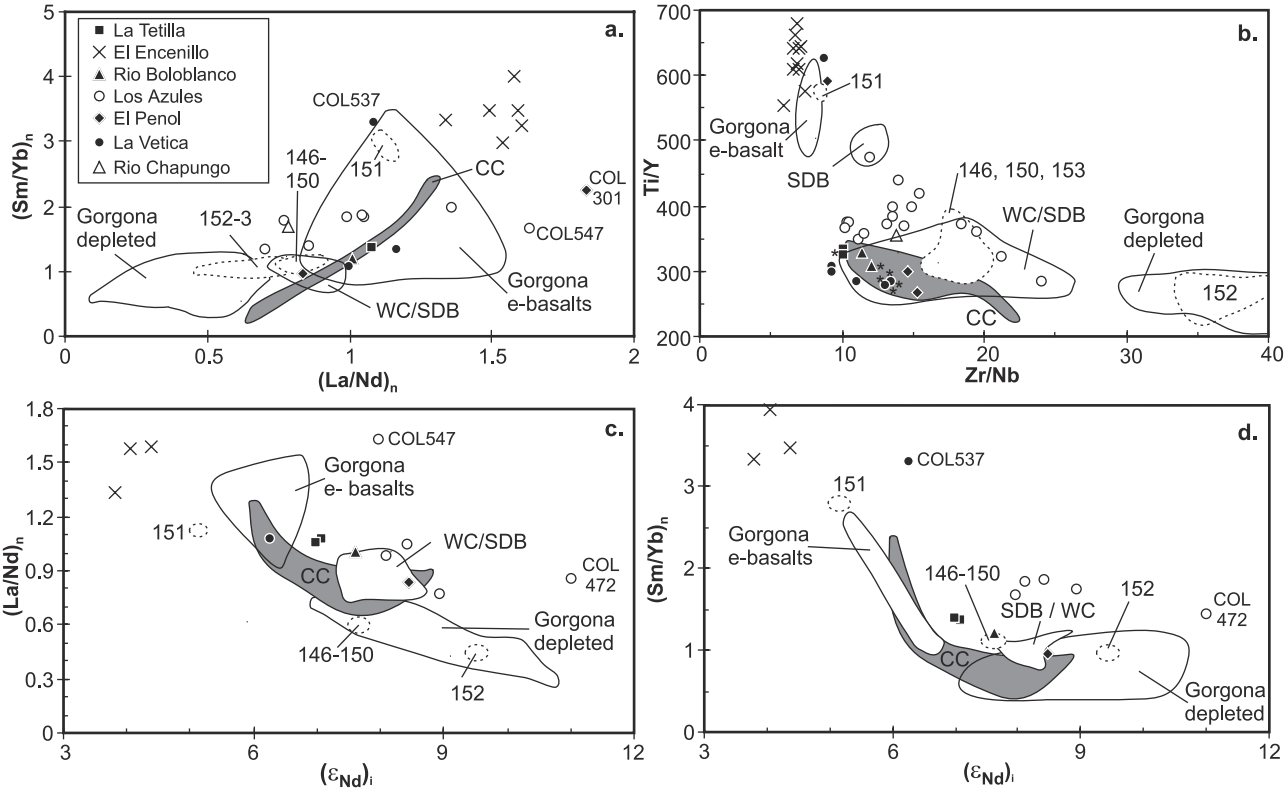

Figure 5. Plots of (a) $(Sm/Yb)_n$ vs. $(La/Nd)_n$; (b) Ti/Y vs. Zr/Nb; (c) $(La/Nd)_n$ vs. $(\varepsilon_{Nd})_i$; (d) $(Sm/Yb)_n$ vs. $(\varepsilon_{Nd})_i$. CC = Colombian Central Cordillera. WC/SDB = Western Cordillera and Serranía de Baudó. Data for Colombia, Curaçao and rest of the CCOP are from *Kerr et al.* [1997a] and *Hauff et al.* [2000a]). Data for Gorgona e-basalts and depleted Gorgona basalts, komatiites and picrites are taken from *Aitken and Echeverría* [1984]; *Kerr et al.*, [1996a]; *Arndt et al.* [1997] and A. C. Kerr et al. (unpublished data, 1995).

[27] The high-MgO El Encenillo rocks, with $(\varepsilon_{Nd})_i$ ranging from +3.6 to +4.1, are the most enriched samples so far analyzed from the CCOP. The El Encenillo picrites contrast markedly with the much more depleted Gorgona komatiites and picrites, which possess much higher $(\varepsilon_{Nd})_i$ (> +9.0). *Alvarado et al.* [1997] and *Hauff et al.* [2000b] have reported similarly enriched picrites ($(\varepsilon_{Nd})_i$ + 4.2 to +5.4), from Tortugal in Costa Rica, which *Alvarado et al.* [1997] proposed were a part of the CCOP. However, the absence of similarly enriched lavas in the rest of the CCOP led *Hauff et al.* [2000b] to suggest that the Tortugal picrites might be a part of the continental Chortis Block. Given the occurrence of obviously oceanic picrites with a very similar elemental and isotopic composition at El Encenillo, we would contend that the Tortugal picrites are indeed a part of the CCOP, as originally proposed by *Alvarado et al.* [1997].

3. Mantle Melting and Sources

[28] Before any assessment of mantle melting and sources can be made, it is necessary to eliminate or reduce the effects of postmelt generation processes, such as fractional crystallization and accumulation of crystals. Modeling of fractional crystallization in the Western and Central Cordillera basalts reveals that from 15 to 9 wt % MgO, olivine and minor Cr-spinel are the only crystallizing phases [*Kerr et al.*, 1997a]. Thus all of the samples from SW Colombia lie on an olivine (fractionation or accumulation) control line, so calculations involving the addition or removal of olivine from parental magmas (of predetermined MgO content) can be used to estimate the concentration of an incompatible element or oxide in the parental magma. The MgO value we have chosen for the parental magma(s) is 15 wt %, and we have calculated the Zr content of each sample at this MgO value. Zr was chosen for this calculation because of its relative immobility and the wide spread of values it displays in the picrites.

[29] The result of this calculation (Zr_{15}) is shown on Figure 7 relative to Nb/Y, $(Sm/Yb)_n$, and $(La/Nd)_n$, i.e., ratios of incompatible trace elements unaffected by the addition or removal of olivine. These ratios were used because each has the potential to reveal something different about either the chemistry or mineralogy of the source region. $(La/Nd)_n$ ratios tell us if the source region is LREE-depleted or -enriched, whereas Nb/Y and $(Sm/Yb)_n$ will signify whether garnet was present in the source region. All three of these incompatible element ratios can provide information on the extent of melting, as can the Zr_{15} values.

[30] Figure 7 also shows the results of our pooled fractional mantle melting calculations, and the findings are summarized in Table 3. We have used sources ranging from depleted mantle to more enriched (primitive) mantle and from garnet lherzolite through a 50:50 spinel-garnet lherzolite mix to a spinel lherzolite; the degree of melting varies

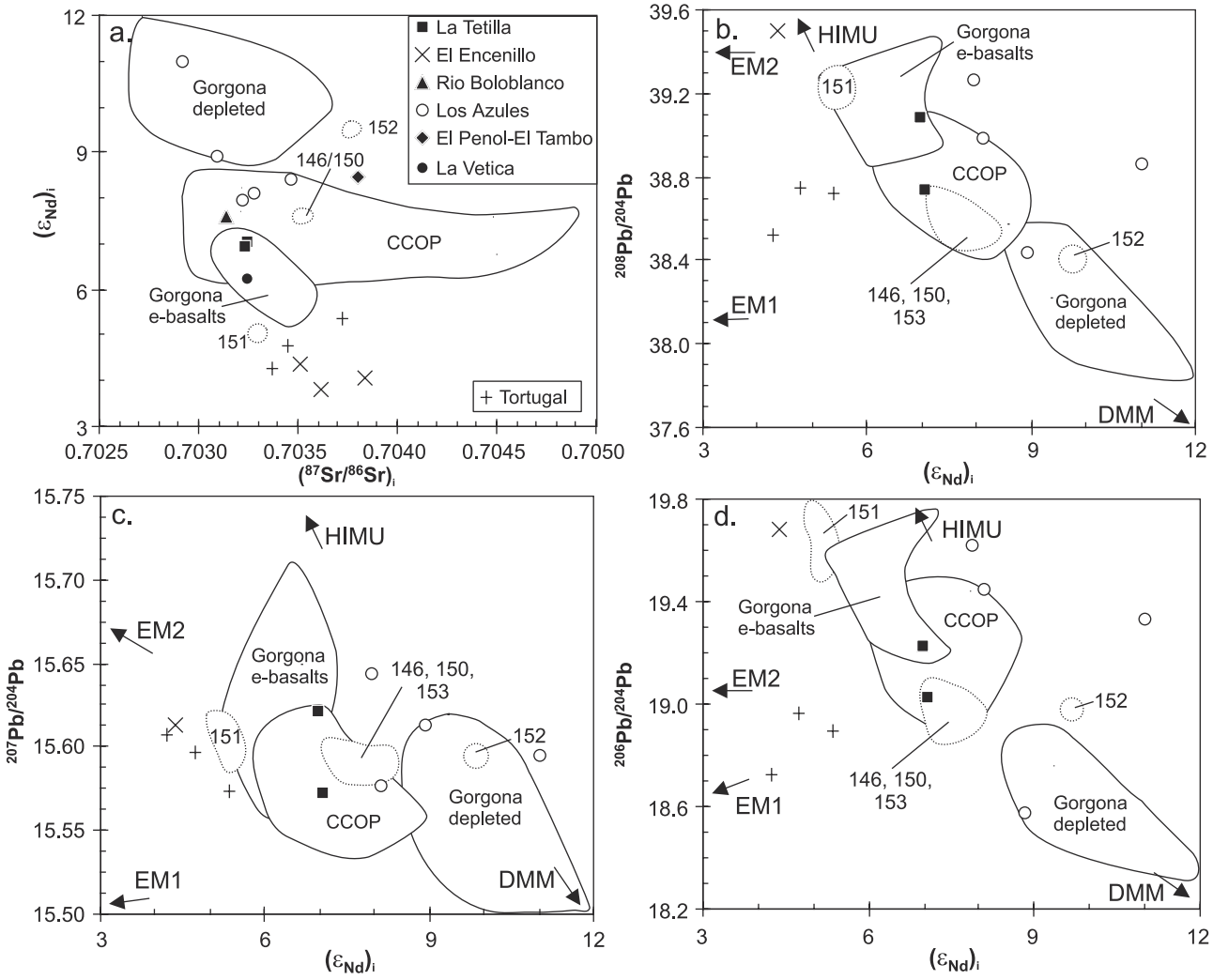

Figure 6. Radiogenic isotope plots for the basalts and picrites from SW Colombia. Data sources are as in Figure 5, in addition to *Dupré and Echeverría* [1984] and *Walker et al.* [1991] (Pb isotopes on Gorgona samples) and *Hauff et al.* [1997; 2000a, 2000b] and *Sinton et al.* [1997] (data from the Nicoya, Tortugal and Leg 15). Mantle end-member compositions are from [*Hart*, 1988].

from 0.5 to 30%. Partition coefficients, mantle mineral proportions, and source compositions used in the modeling are taken from *McKenzie and O'Nions* [1991]. The modeled melt compositions plotted on Figure 7 represent melting at discrete depths within the plume; no attempt has been made to pool melts from various depths in the mantle. The El Encenillo rocks (type 1; Figure 3), despite possessing $(Sm/Yb)_n > 1$ and $Nb/Y > 0.8$, appear not to be derived from a pure garnet lherzolite source region (>90 km in a hot mantle plume [*Watson and McKenzie*, 1991]). Rather, the source region of these magmas comprised mostly spinel lherzolite with smaller amounts of garnet lherzolite (Figure 7c and Table 3); it was enriched relative to depleted MORB-source mantle and under went <5% melting to form the El Encenillo magmas (Figures 7a and 7b).

[31] Samples with $(La/Nd)_n > 0.1$, $(Sm/Yb)_n = 2–3$ and $Nb/Y = 0.4–0.8$ (type 2; Figure 3) must also contain some garnet in their mantle source region (Figure 7c and Table 3). The compositions of some of these rocks (with $Zr_{15} = 58–80$, $(La/Nd)_n = 1.15–1.80$, and $Nb/Y = 0.50–0.65$) cannot be modeled by simple melting of any of the source materials (Figures 7a and 7b) but can be explained by mixing between very small degree (<3%) melts of a garnet lherzolite source region and larger degree melts (>20%) of a shallower source region. Thus this type appears to represent the products of mixing within a mantle melt column.

[32] The rocks which contain $(La/Nd)_n = 0.9–1.4$, $(Sm/Yb)_n = 1.5–2.0$, and $Nb/Y = 0.1–0.4$ (type 3; Figure 3) require a more depleted source region than types 1 and 2, and this is borne out by the higher $(\varepsilon Nd)_i$ and the lower $(La/Nd)_n$ of these samples (Figure 7b). The mantle source region also contains more spinel (Figures 7b and 7c and Table 3); it was therefore shallower and underwent a greater degree of melting (15–20%) than types 1 and 2.

[33] The most depleted rocks, i.e., samples from Los Azules and Sites 146, 150, 151, and 153 (type 4; Figure 3) with $(La/Nd)_n = 0.9–1.4$, $(Sm/Yb)_n = 1.5–2.0$, and $Nb/Y = 0.1–0.4$, are best modeled by a LREE-depleted source region (Figure 7a) containing only a small proportion of garnet lherzolite (Figures 7a, 7b, and 7c and Table 3). The extent of melting is also relatively high at 15–20%.

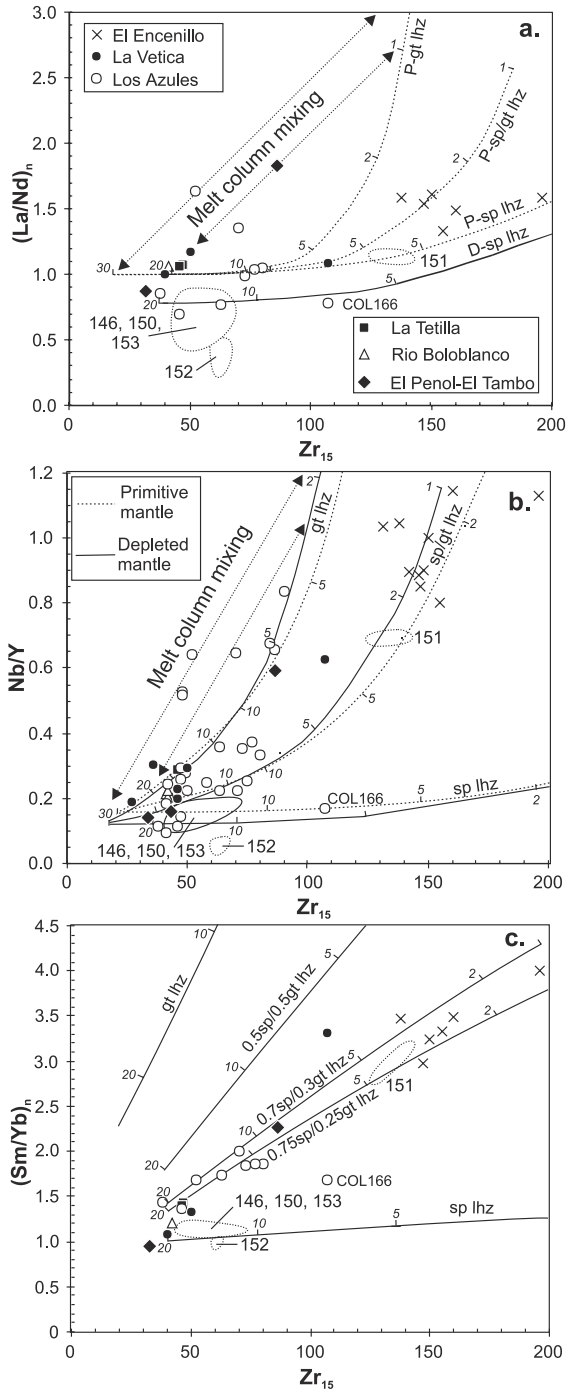

Figure 7. Modeling results from pooled fractional melting calculations for various possible mantle source regions. Numbered ticks on the melting curves indicate percentage of partial melting (see text and Table 3 for more details). Zr_{15} indicates the Zr content has been corrected to 15% MgO by the addition or removal of olivine (see text for more details). Abbreviations: sp lhz – spinel lherzolite; gt lhz – garnet lherzolite, P – primitive mantle; D – depleted mantle. Numbers beside spinel and garnet lherzolite indicate the proportion of spinel to garnet lherzolite in the source. Where no numbers are given the proportion of garnet to spinel lherzolite is 50:50. On Figure 7c the three modeled source compositions are all 50:50 mixtures of depleted and primitive mantle.

[34] Thus the four magma types identified in this study represent progressively more extensive melting at shallower depths. One can envisage a streaky plume with a more depleted and refractory matrix that makes up >95% of the plume but which contains more enriched and fusible streaks or blobs [cf. *Kerr et al.*, 1995; *Arndt et al.*, 1997]. Deeper, and so less extensive, melting would preferentially sample the more enriched streaks (El Encenillo; Type 1). Further ascent, along with the concomitant decompression of this source region, would result in more extensive melting. The enriched component would therefore become diluted as the depleted component contributes a greater proportion to the melt. Alternatively, the mantle which ascends to shallower depths may be intrinsically more depleted, having had most of its enriched components extracted at depth. Mixing of the deep enriched melts with the shallower more extensive melts in the melt column could produce the type 2 magmas. The shallowest melting (type 4) occurs in those parts of the plume which have already had largely all of the enriched components extracted from them. The overall depleted signature of the samples with <0.9 $(La/Nd)_n$, combined with the moderate degrees of melting required, favors this model as opposed to one in which the enriched component is present in the source but its signature is swamped by extensive melting of the depleted matrix.

4. Mantle Plume Heterogeneity

[35] It has been known for some time that different mantle plumes can possess different chemical and isotopic signatures: EM1, EM2, HIMU, etc. [cf. *Hart*, 1988; *Weaver*, 1991]. However, in addition to this interplume chemical variation, there can also be a significant intraplume heterogeneity [*Hémond et al.*, 1993; *White et al.*, 1993; *Kerr et al.*, 1995]. Furthermore, there has been an increasing realization that mantle plumes, once regarded as being derived from a long-term enriched source [cf. *Hart*, 1988], can possess significant long-term depleted component(s) chemically distinct from depleted mid-ocean ridge basalt (MORB) mantle (DMM) [e.g., *Thirlwall et al.*, 1994; *Kerr et al.*, 1995; *Arndt et al.*, 1997; *Fitton et al.*, 1997; *Nowell et al.*, 1998; *Kempton et al.*, 2000].

[36] In relation to the picrites and high-MgO basalts from SW Colombia, it is first of all important to ascertain if all the lavas (and, in particular, the more depleted ones) have indeed been derived from a mantle plume. A plot of log Nb/Y against log Zr/Y (devised by *Fitton et al.* [1997]) has thus far shown itself to be a robust discriminant between basalts derived from a DMM source region and those derived from both enriched and depleted plume source regions. On Figure 8 all plume-derived lavas from Iceland plot between two "tramlines." *Kerr et al.* [1997a] have previously shown that oceanic plateau basalts from Colombia and from the Ontong Java Plateau also plot within these tramlines. With the exception of one sample plotting above the tramlines, all of the new data for the picrites and basalts from SW Colombia fall within the tramlines and are thus interpreted as being derived from a mantle plume source region (Figure 8). It is worth noting that even the more depleted Los Azules group samples ($(La/Nd)_n < 1$; $(\varepsilon_{Nd})_i > +8.5$) are not apparently derived from a DMM source region, even though they are depleted relative to bulk earth

Table 3. Summary of Mantle Melt Modeling

	$(La/Nd)_n$	$(Sm/Yb)_n$	Nb/Y	Conclusions
Type 1				
Source lherzolite	garnet/spinel	spinel with minor garnet	garnet/spinel	50/50; garnet/spinel
Enriched/depleted	enriched	[a]	[a]	enriched
Melting/mixing	3–4% melting	3–5% melting	2–4% melting	3–5% melting
Type 2				
Source lherzolite	garnet	spinel with minor garnet	garnet	garnet with minor spinel
Enriched/depleted	enriched	[a]	enriched	enriched
Melting/mixing	mixing of a 30% melt with <5% melt	mixing (possible melting 10–15%)	mixing of a 30% melt with <5% melt	mixing of a 30% melt with <5% melt
Type 3				
Source lherzolite	[b]	spinel with minor garnet	50/50; garnet/spinel	50/50; garnet/spinel
Enriched/depleted	depleted-enriched mix	[a]	[a]	depleted-enriched mix
Melting/mixing	10–15% melting (possible mixing)	15–20% melting	10–20% melting (possible mixing)	15–20% melting
Type 4				
Source lherzolite	[b]	spinel with minor garnet	spinel with minor garnet	spinel with minor garnet
Enriched/depleted	depleted	[a]	depleted	depleted
Melting/mixing	10–15% melting	>15% melting	10–20% melting	15–20 %

[a] $(Sm/Yb)_n$ and Nb/Y reveal little about the level of enrichment of the source region.
[b] $(La/Nd)_n$ reveals little about the mineralogy of the source region at large degrees of melting.

(positive $(\varepsilon_{Nd})_i$; Figure 6a). Thus all of the heterogeneity observed in the picrites and high-MgO basalts from SW Colombia appears to be derived from the mantle plume source region. This lends further weight to proposals which have suggested that mantle plume source regions are markedly heterogeneous [*Hémond et al.*, 1993; *Thirlwall et al.*, 1994; *Kerr et al.*, 1995; *Kempton et al.*, 2000].

[37] *Hauff et al.* [2000a] also recognized two end-members within the plume responsible for the CCOP, a HIMU-like component and a more depleted, DMM-like source, which was suggested to be either recycled lower oceanic crust or MORB source mantle. However, as we have seen from trace element considerations (Figure 8), this source cannot be MORB source mantle and must be similar to the depleted Icelandic mantle of *Fitton et al.* [1997] and *Kempton et al.* [2000]. Following the reasoning of *Kerr et al.* [1995], this source is probably derived from recycled oceanic lithosphere (unlike HIMU, which is believed to be derived from relatively more enriched recycled oceanic crust [*Hofmann and White*, 1982; *Phipps Morgan and Morgan*, 1999]). Depleted oceanic lithosphere as a potential source of (recycled) material was not discussed by *Hofmann and White* [1982], who suggested that oceanic lithosphere separated from the oceanic crust during subduction and was mixed back into the upper mantle.

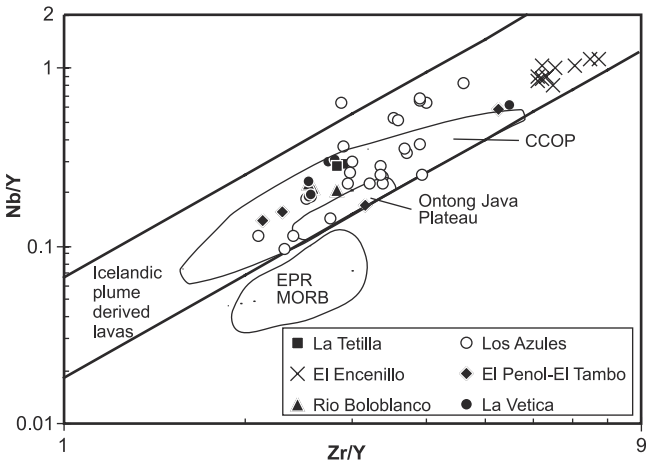

Figure 8. Log-log plot of Nb/Y vs. Zr/Y (after *Fitton et al.*, 1997). All samples derived from the Icelandic mantle plume fall within the tramlines, whereas East Pacific Rise MORB [from *Mahoney et al.*, 1994] plot below this field. WC/SDB/CC-data for basalts from the Western Cordillera; Central Cordillera and the Serranía de Baudó of Colombia. Data sources are as in Figures 5–6.

[38] As noted above, in addition to this depleted plume component, and the HIMU-like component, the lowest $(\varepsilon_{Nd})_i$ values thus far recorded in the CCOP: +3 to +4 in the picrites from El Encenillo and +4 to +5 in the Tortugal picrites, Costa Rica [*Hauff et al.*, 2000b], provide evidence of a third component in the CCOP plume. This source region is characterized by $^{206}Pb/^{204}Pb$ = 19.1 to 19.5, $^{207}Pb/^{204}Pb$ = 15.60 to 15.65, and $(\varepsilon_{Nd})_i$ = +3 to −1 and is strongly suggestive of an EM2 (or possibly an EM1) component in the plume. The source of EM2 has been ascribed to subducted terrigenous sediment [*Hart*, 1988; *Weaver*, 1991].

[39] The lower $(\varepsilon_{Nd})_i$ of the Site 151 basalts and some of the Gorgona e-basalts provide evidence that this component was probably widespread throughout the plume head. The close spatial association of lavas with depleted and enriched signatures in the CCOP gives us some idea of the length scale of plume heterogeneity. The El Encenillo and Los Azules lavas are <50 km apart, suggesting that the heterogeneity within the plume is present on a scale of tens of kilometers. Locally, however, it appears that the heterogeneity exists at much shorter length scales (<10 km) within the plume head, since the enriched and depleted lavas from Gorgona occur within a kilometer of each other.

5. Conclusions

[40] The picrites and picritic basalts of SW Colombia have been derived from a mantle plume and are part of the CCOP. Fractionation and accumulation of olivine have been the main magmatic processes and account for the wide range in MgO contents. We calculate that the parental magmas contained between 14 and 18 wt % MgO.

[41] CCOP rocks from the Central Cordillera of Colombia have yielded $^{40}Ar/^{39}Ar$ step-heating ages of 93-89 Ma, and so the lavas are similar in age to those of the Western Cordillera of Colombia. The high-MgO rocks of the Central Cordillera and the basalts from DSDP Leg 15 display a considerable degree of heterogeneity, both in terms of trace element and isotopic ratios, which enable them to be subdivided into four different magma types.

[42] Modeling of the mantle melting process suggests that the plume can be envisaged as comprising fusible enriched streaks set in a more depleted and refractory matrix. Deep and therefore small-degree (<3%) melting, mostly within the stability field of garnet lherzolite, preferentially samples the most fusible components, producing the most enriched lavas ($(La/Nd)_n$ >1 $(\varepsilon_{Nd})_i$ +3 to +4). Shallower and more extensive melting (10–20%), which occurs after the enriched component has been largely removed at depth, will produce the more depleted magma types. Modeling shows that the trace element compositions of some of the lavas from the Central Cordillera have been produced by mixing within a melt column between trace element-enriched, small-degree melts from deep in the mantle and more depleted, larger degree melts from shallower depths.

[43] Although many of the lavas from the study possess evidence of derivation from a time-integrated depleted source region, Nb/Y and Zr/Y systematics reveal that this source region is not DMM but is rather a depleted source region intrinsic to the plume. The discovery of CCOP lavas with $(\varepsilon_{Nd})_i$ +3 to +4 and $^{206}Pb/^{204}Pb$ values ranging from 19.1 to 19.5 and $^{207}Pb/^{204}Pb$ from 15.50 to 15.65 is suggestive of an enriched mantle (EM2 or possibly EM1) component within the plume.

[44] **Acknowledgments.** These studies were supported by Natural Environment Research Council (UK) through grants GR3/8984 and GR9/583A (to J.T.). We wish to thank INGEOMINAS for logistical support during fieldwork in Colombia. Pat Thompson, Roz White, Ray Kent, and Andy Saunders as always provided stimulating geochemical discussions. Constructive reviews from Folkmar Hauff, Jun Korenaga, and Garret Ito are much appreciated, as was the editorial assistance of Francis Albarede. This paper represents NERC Isotope Geosciences Laboratory publication 469.

References

Aitken, B. G., and L. M. Echeverría, Petrology and geochemistry of komatiites and tholeiites from Gorgona Island, Colombia, *Contrib. Mineral. Petrol.*, *86*, 94–105, 1984.

Alvarado, G. E., P. Deyner, and C. W. Sinton, The 89 Ma Tortugal komatiitic suite, Costa Rica: Implications for a common origin of the Caribbean and eastern Pacific region from a mantle plume, *Geology*, *25*, 439–442, 1997.

Arndt, N. T., A. C. Kerr, and J. Tarney, Differentiation in plume heads: The formation of Gorgona komatiites and basalts, *Earth Planet. Sci. Lett.*, *146*, 289–301, 1997.

Dalrymple, G. B., D. A. Clague, T. L. Vallier, and H. W. Menard, $^{40}Ar/^{39}Ar$ age, petrology, and tectonic significance of some seamounts in the Gulf of Alaska, in *Seamounts, Islands, and Atolls*, *Geophys. Monogr. Ser.*, vol. 43, edited by B. H. Keating, et al., pp. 297–315, AGU, Washington, D. C., 1988.

Donnelly, T. W., W. Melson, R. Kay, and J. J. W. Rogers, Basalts and dolerites of late Cretaceous age from the central Caribbean, *Initial Rep. Deep Sea Drill. Proj.*, *15*, 989–1004, 1973.

Donnelly, T. W., et al., History and tectonic setting of Caribbean magmatism, in *The Geology of North America*, *vol. H*, *The Caribbean Region*, edited by G. Dengo and J. E. Case, pp. 339–374, Geol. Soc. of Am., Boulder, Colo., 1990.

Duncan, R. A., and R. B. Hargraves, $^{40}Ar/^{39}Ar$ geochronology of basement rocks from the Mascarene Plateau, Chagos Bank, and Maldives Ridge, *Proc. Ocean Drill. Program Sci. Results*, *115*, 43–52, 1990.

Duncan, R. A., and L. G. Hogan, Radiometric dating of young MORB using the $^{40}Ar/^{39}Ar$ incremental heating method, *Geophys. Res. Lett.*, *21*, 1927–1930, 1994.

Dupré, B., and L. M. Echeverría, Pb Isotopes of Gorgona Island (Colombia): Isotopic variations correlated with magma type, *Earth Planet. Sci. Lett.*, *67*, 186–190, 1984.

Fitton, J. G., A. D. Saunders, M. J. Norry, B. S. Hardarson, and R. N. Taylor, Thermal and chemical structure of the Iceland plume, *Earth Planet. Sci. Lett.*, *153*, 197–208, 1997.

Frey, F. A., et al., Origin and evolution of a submarine large igneous province: The Kerguelen Plateau and Broken Ridge, southern Indian Ocean, *Earth Planet. Sci. Lett.*, *176*, 73–89, 2000.

Hart, S. R., Heterogeneous mantle domains: Signatures, genesis and mixing chronologies, *Earth Planet. Sci. Lett.*, *90*, 273–296, 1988.

Hauff, F., K. Hoernle, H.-U. Schmincke, and R. Werner, A mid Cretaceous origin for the Galápagos hotspot: Volcanological, petrological, and geochemical evidence from Costa Rican oceanic crustal segments, *Geol. Rundsch.*, *86*, 141–155, 1997.

Hauff, F., K. Hoernle, G. Tilton, D. W. Graham, and A. C. Kerr, Large volume recycling of oceanic lithosphere over short time scales: Geochemical constraints from the Caribbean Large Igneous Province, *Earth Planet. Sci. Lett.*, *174*, 247–263, 2000a.

Hauff, F., K. Hoernle, P. van den Bogaard, G. Alvarado, and D. Garbe-Schönberg, Age and geochemistry of basaltic complexes in western Costa Rica: Contributions to the geotectonic evolution of Central America, *Geochem. Geophys. Geosyst.*, *1*(article), 1999GC000020[10,051 words], 2000b.

Hémond, C., N. T. Arndt, U. Lichtenstein, A. W. Hofmann, N. Oskarsson, and S. Steinthorsson, The heterogeneous Iceland plume: Nd-Sr-O isotopes and trace element constraints, *J. Geophys. Res.*, *98*, 15,833–15,850, 1993.

Hofmann, A. W., and W. M. White, Mantle plumes from ancient oceanic crust, *Earth Planet. Sci. Lett.*, *57*, 421–436, 1982.

Hurfurd, A. J., and K. Hammerschmidt, $^{40}Ar/^{39}Ar$ and K-Ar dating of the Bishop and Fish Canyon Tuffs: Calibration ages for fission-track dating standards, *Chem. Geol.*, *58*, 23–32, 1985.

Kempton, P. D., Common Pb chemical procedures for silicate rocks and minerals, methods of data correction and an assessment of data quality at the NERC Isotope Geosciences Laboratory, *NIGL Rep. Ser. 78*, 26 pp., NERC Isotope Geosci. Lab., Keyworth, England, 1995.

Kempton, P. D., J. G. Fitton, A. D. Saunders, G. M. Nowell, R. N. Taylor, and B. S. Hardarson, The Iceland plume in space and time: A Sr-Nd-Pb-Hf study of the North Atlantic Rifted Margin, *Earth Planet. Sci. Lett.*, *177*, 255–271, 2000.

Kerr, A. C., A. D. Saunders, J. Tarney, N. H. Berry, and V. L. Hards, Depleted mantle plume geochemical signatures: No paradox for plume theories, *Geology*, *23*, 843–846, 1995.

Kerr, A. C., G. F. Marriner, N. T. Arndt, J. Tarney, A. Nivia, A. D. Saunders, and R. A. Duncan, The petrogenesis of komatiites, picrites and basalts from the Isle of Gorgona, Colombia: New field, petrographic and geochemical constraints, *Lithos*, *37*, 245–260, 1996a.

Kerr, A. C., J. Tarney, G. F. Marriner, G. T. Klaver, A. D. Saunders, and M. F. Thirlwall, The geochemistry and petrogenesis of the late-Cretaceous picrites and basalts of Curaçao, Netherlands Antilles: A remnant of an oceanic plateau, *Contrib. Mineral. Petrol.*, *124*, 29–43, 1996b.

Kerr, A. C., G. F. Marriner, J. Tarney, A. Nivia, A. D. Saunders, M. F. Thirlwall, and C. W. Sinton, Cretaceous basaltic terranes in western Colombia: Elemental, chronological and Sr-Nd constraints on petrogenesis, *J. Petrol.*, *38*, 677–702, 1997a.

Kerr, A. C., J. Tarney, G. F. Marriner, A. Nivia, and A. D. Saunders, The Caribbean-Colombian Cretaceous igneous province: The internal anatomy of an oceanic plateau, in *Large Igneous Provinces*, *Geophys. Monogr. Ser.*, vol. 100, edited by J. J. Mahoney and M. F. Coffin, pp. 45–93, AGU, Washington, D. C., 1997b.

Kerr, A. C., J. Tarney, A. Nivia, G. F. Marriner, and A. D. Saunders, The internal structure of oceanic plateaus: Inferences from obducted Cretaceous terranes in western Colombia and the Caribbean, *Tectonophysics*, *292*, 173–188, 1998.

Korenaga, J., and P. B. Kelemen, Major element heterogeneity in the mantle source of the North Atlantic igneous province, *Earth Planet. Sci. Lett.*, *184*, 251–268, 2000.

Lapierre, H., et al., Multiple plume events in the genesis of the peri-Caribbean Cretaceous oceanic plateau province, *J. Geophys. Res.*, *105*, 8403–8421, 2000.

Mahoney, J. J., M. Storey, R. A. Duncan, K. J. Spencer, and M. Pringle, Geochemistry and age of the Ontong Java Plateau, in *The Mesozoic Pacific: Geology, Tectonics and Volcanism*, *Geophys. Monogr Ser.*, vol. 77, edited by M. S. Pringle et al., pp. 233–261, AGU, Washington, D. C., 1993.

Mahoney, J. J., J. M. Sinton, J. D. Macdougall, K. J. Spencer, and G. W. Lugmair, Isotope and trace element characteristics of a super-fast spreading ridge: East Pacific Rise, 13–23°S, *Earth Planet. Sci. Lett.*, *121*, 173–193, 1994.

McCourt, W. J., J. A. Aspden, and M. Brook, New geological and geochronological data from the Colombian Andes: Continental growth by multiple accretion, *J. Geol. Soc. London*, *141*, 831–845, 1984.

McKenzie, D., and R. K. O'Nions, Partial melt distributions from inversion of rare earth element concentrations, *J. Petrol.*, *32*, 1021–1091, 1991.

Millward, D., G. F. Marriner, and A. D. Saunders, Cretaceous tholeiitic volcanic rocks from the Western Cordillera of Colombia, *J. Geol. Soc. London*, *141*, 847–860, 1984.

Neal, C. R., J. J. Mahoney, L. W. Kroenke, R. A. Duncan, and M. G. Petterson, The Ontong Java Plateau, in *Large Igneous Provinces*, *Geophys. Monogr. Ser*, vol. 100, edited by J. J. Mahoney and M. F. Coffin, pp. 183–216, AGU, Washington, D. C., 1997.

Nivia, A., The Bolívar mafic-ultramafic complex, SW Colombia: The base of an obducted oceanic plateau, *J. S. Am. Earth Sci.*, *9*, 59–68, 1996.

Nowell, G. M., P. D. Kempton, S. R. Noble, J. G. Fitton, A. D. Saunders, J. J. Mahoney, and R. N. Taylor, High precision Hf isotope measurements of MORB and OIB by thermal ionisation mass spectrometry: Insights into the depleted mantle, *Chem. Geol.*, *149*, 211–233, 1998.

Phipps Morgan, J., and W. J. Morgan, Two stage melting and the geochemical evolution of the mantle: A recipe for mantle plum-pudding, *Earth Planet. Sci. Lett.*, *170*, 215–239, 1999.

Royse, K. R., P. D. Kempton, and D. P. F. Darbyshire, Procedure for the analysis for rubidium-strontium and samarium-neodymium isotopes at the NERC Isotope Geosciences Laboratory, *NIGL Rep. Ser. 121*, 28 pp., NERC Isotope Geosci. Lab., Keyworth, England, 1998.

Sinton, C. W., R. A. Duncan, and P. Denyer, Nicoya Peninsula, Costa Rica: A single suite of Caribbean oceanic plateau magmas, *J. Geophys. Res.*, *102*, 15,507–15,520, 1997.

Sinton, C. W., R. A. Duncan, M. Storey, J. Lewis, and J. J. Estrada, An oceanic flood basalt province within the Caribbean plate, *Earth Planet. Sci. Lett.*, *155*, 221–235, 1998.

Sinton, C. W., H. Sigurdsson, and R. A. Duncan, Geochronology and petrology of the igneous basement at the lower Nicaraguan Rise, Site 1001, *Proc. Ocean Drill. Program Sci. Results*, *165*, 233–236, 2000.

Spadea, P., E. Espinosa, and A. Orrego, High-Mg extrusive rocks from the Romeral zone ophiolites in the south western Colombian Andes, *Chem. Geol.*, *77*, 303–321, 1989.

Sun, S.-S., and W. F. McDonough, Chemical and isotopic systematics of oceanic basalts: Implications for mantle composition and processes, in *Magmatism in the ocean basins*, edited by A. D. Saunders and M. J. Norry, *Geol. Soc. Spec. Publ.*, 42, 313–345, 1989.

Thirlwall, M. F., B. G. J. Upton, and C. Jenkins, Interaction between continental lithosphere and the Iceland plume—Sr-Nd-Pb isotope geochemistry of Tertiary basalts, NE Greenland, *J. Petrol.*, *35*, 839–879, 1994.

Todt, W., R. A. Cliff, A. Hanser, and A. W. Hofmann, Re-calibration of NBS lead standards using a $^{202}Pb + {}^{205}Pb$ double spike, *Terra Abstr.*, *5*, 396, 1993.

Walker, R. J., L. M. Echeverría, S. B. Shirey, and M. F. Horan, Re-Os isotopic constraints on the origin of volcanic rocks, Gorgona Island, Colombia: Os isotopic evidence for ancient heterogeneities in the mantle, *Contrib. Mineral. Petrol.*, *107*, 150–162, 1991.

Weaver, B. L., The origin of ocean island basalt end-member compositions: Trace element and isotopic constraints, *Earth Planet. Sci. Lett.*, *104*, 381–397, 1991.

Weis, D., Y. Bassias, I. Gautier, and J.-P. Mennessier, Dupal anomaly in existence 115 Ma ago: Evidence from isotopic study of the Kerguelen Plateau (South Indian Ocean), *Geochim. Cosmochim. Acta*, *53*, 2125–2131, 1989.

White, W. M., A. R. McBirney, and R. A. Duncan, Petrology and geochemistry of the Galápagos Islands: Portrait of a pathological mantle plume, *J. Geophys. Res.*, *98*, 19,533–19,563, 1993.

R. A. Duncan, College of Oceanography, Oregon State University, Corvallis, OR 97331, USA. (rduncan@oce.orst.edu)

P. D. Kempton, NERC Isotope Geosciences Laboratory, c/o British Geological Survey, Keyworth, Nottingham, NG12 5GG, UK. (p.kempton@nigl.nerc.ac.uk)

A. C. Kerr, Department of Earth Sciences, Cardiff University, P.O. Box 914, Cardiff, Wales, CF10 3YE, UK. (kerra@cf.ac.uk)

G. F. Marriner, Department of Geology, Royal Holloway, University of London, Egham, Surrey, TW20 0EX, UK. (G.Marriner@btinternet.com)

A. Nivia, Ingeominas–Regional Pacifico, AA 9724, Cali, Colombia, USA. (anivia@calipso.com.co)

P. Spadea, Università Degli Studi di Udine, Dipartimento di Georisorse E Territorio, via Cotonificio N. 114, 33100, Udine, Italy. (spadea@hydrus.cc.uniud.it)

J. Tarney, Department of Geology, University of Leicester, University Road, Leicester, LE1 7RH, UK. (art@le.ac.uk)